Research Article

Mesoscopic irreversible thermodynamics of morphological evolution kinetics of helical conformation in bioproteins 'DNA' under the isothermal isobaric conditions

Tarik Omer Ogurtani[1]* and Ersin Emre Oren[2]

[1]Department of Metallurgical and Materials Engineering, Middle East Technical University, 06690, Ankara, Turkey

[2]Bionanodesign Laboratory, Department of Biomedical Engineering, TOBB University of Economic and Technology, 06560 Ankara, Turkey

Check for updates

OPEN ACCESS

Abstract

The morphological evolution kinetics and instabilities of alpha helical peptide 3.6_{13}, which involves large amount of stored torsional elastic deformation energy (3-40 eV/ molecule), is formulated by the variational method based on the connection between the rates of internal entropy production and the changes in the global Gibbs free energy, assuming that one has isobaric irreversible processes under the isothermal conditions. The present mesoscopic nonequilibrium thermodynamic approach relies on the fact that the global Gibbs free energy of helical conformation involves not only the bulk Gibbs free energy of the amino-acid back bone structure but also the interfacial Gibbs free energy of the enclosing cylindrical shell or the cage associated with the side-wall molecular branches, and their interactions with the immediate surroundings. The proposed variational analysis applied directly on the proposed macro-model has furnished a nonlinear integral equation in terms of the normalized and scaled internal and external variables. This allows us to track down the motion of the total pitch height of the alpha polypeptide along the well-defined trajectories in the displacement-time space, dictated not only by the initial configuration of the helix but also through the gradients of the global Gibbs free energy of the strained helical conformation as the main driving force. In the negative manifold, there is a well-defined region below the dynamic instability regime, in which the helical conformation can evolve towards the nonequilibrium stationary states by expanding, or contracting, depending upon whether the interfacial free energy and/or the applied stress system are below or above the well-defined thresholds level dictated by the initial pitch height. The highest life time may be realized along that trajectory, which follows up the threshold level of the interfacial specific Gibbs free energy, which is g_s = -315 erg/cm². In the upper region of the negative manifold, the helical conformations are driven by the very large applied uniaxial tension or the negative pressure induced by the thermal expansion, in the range of p > 1GPa and/or the strong negative interfacial free energies [3-4 pH] or their combinations, they show strong kinematic instabilities, which can cause not only the accelerated unfolding phenomenon but also cause large extensions that end up with the catastrophic decimations by ruptures and fragmentations. In the positive manifold, the aging behavior of the polypeptide follows up a S-shape path having rather speedy aging behavior compared to the negative manifold, which is separated from by a well-defined boundary, which represents the isochoric path having longest relaxation times, which can be achieved with great stability. Finally, one could attempt to estimate the upper limit of the relaxation time of aging for the modern hominin, from samples of exceptional preservations, relying on the present nonequilibrium theory as well as on the very limited knowledge on the post-mortem DNA and the present pitch heights of the modern hominin, which is found to be about 25,840 yrs, with a life expectation of 451,800 yrs. These figures are very close to those calculated for Neanderthals (SH), which are found to be 31,820 yrs and 499,100 yrs, respectively.

Introduction

Our main interest in dealing with the morphological evolution kinetics of polypeptides is based on the experimental observations that the acidity pH of the embedding aqua solutions dramatically controls the stability and as well as the decimation of the alpha-polypeptides exposed to the constant hydrostatic pressure or the uniaxial tension and compression [1,2]. Similarly, the mechanics of the bioprotein materials having helical conformations still remain in great extend unknown [3-5]. Most of the present theories are based on the ad hoc phenomenological theory proposed by Bell [6], that relies on the well-known transition state or the activation complex theory of chemical kinetics modified by the applied stress systems, which is extensively used in phase transformations in physical metallurgy and materials science [7,8]. Similarly, the role of the stored elastic torsional energy during the formation of the helical conformation is miscalculated or completely over looked because of the lack of knowledge in this highly controversial field of elasticity [9]. Ackbarow, et al. [3], derived their rate equation for the bond breaking using some ad hoc mechanical arguments relying on the *activated-complex theory* "transition state theory" [7] modified originally by Bell [6] to take care of the effect of the applied stress on the Gibbs free energy barrier, while he was dealing with the adhesion of cells to cells. In later stage, they switched to so call the hierarchical Bell model, which deals with statistics of the chemical bonds based on the robustness parameter postulated by Kitano, [10], whether they are breaking sequentially or collectively. The experiments performed by Ackbarow, et al. [3], show that the fast deformation mode [$v = 10$ m/s] compared to the slow deformation, which is done with pulling speed of 0.1 m/s, requires much higher applied force intensity in order to replicate the similar force–strain pattern with an almost factor of four zooming. That means there is anomalous strain rate sensitivity, where the connection between the applied force and the displacement velocity is linear, which mimics the typical Stokian-Law, and but not the Hookean linear elasticity. They speculated that this factor of four of correlation is closely associated with the numbers of broken hydrogen bonds [HB] of amino acid residues during the pulling testing, therefore there should be 3-4 parallel HB per turn are favorable in the light of the bioprotein mechanical and thermodynamic stability. Their claim conflicts with the structure of alpha-polypeptides in the literature especially with the experimental results presented by Idiris, et al. [1], which are completely in accord with the predictions of our irreversible thermodynamic theory that employs the unusual torque term advocated by Ogurtani [9] for the helical conformations. Furthermore, according to Pauling, et al. [11], there should be only two hydrogen bounding in whole alpha-helix conformation designated by 3.6_{13}, where 13 is the total number of atomic species present in each amino acid residue enclosing a single turn including hydrogen atom. This argument urged Pauling to realize that the helix has 3.6_{13} residues per turn, with a hydrogen bond between the C = O of the residue n on top coil and the N-H of the residue $n + 4$ on bottom coil.

In all these theories, not only the unusual mechanical behavior of the helical conformation, due to the non-vanishing "residual" torque [9] acting on the amino-acid backbone structure, is over looked, but also the physico-chemical interactions with its surroundings through the branching molecular residues, which may cause denaturation [1,12] are excluded in their formulations. Kojima, et al. [13], obtained the tensile strength and Young modulus of a single acting fiber, respectively, as 600 pN (6×10^{-5} dyne) and 2.5 GPA. Radmacher, et al. [14], measured the Young modulus of compressed Iysozyme molecules on a mica surface, and found about 0.5 GPA. Afin, et al. [15,16] improved the AFM-based method, and obtained Young's modulus for immobilized carbon anhydrase molecules as 70-80 MPa. Nano mechanical properties of vimentin intermediate filament dimmers have been studied by Qin, et al. [17], who obtained force-engineering strain diagram showing three distinct sections. The first regime shows a typical linear elastic behavior with a Young's modulus of 600 ± 300 MPa. The second regime corresponds to the plateau with a slight increase of the force about 1.079 pN per %, that continuous till the α-helical protein is completely unfolded. In the third regime, the filament stiffness becomes appreciable. Their interpretation on the H-bonds breaking hypothesis is not justified by their tensile deformation test, which doesn't give any clue for the existence of the sharp upper yield point followed up sudden drop in the stress, and then comes the plateau region. The Young modulus of a peptide surfactant film self-assembled at the air water interface, which is designated as AM1 is experimentally determined by Middelberg, et al. [18], and it is found that it can be switched, reversibly, from a high- to low-elasticity states (E = 80 MPa for AM1 and switching to E < 20MPa), with rapid loss of emulsion and foam stability. In all these mechanical behavior studies no one has yet mentioned the role of the torsional and bending deformation of helical conformation, and the associated stored elastic energy, which is the inherent property of the helix at rest, and the main reason for its spring like elastic behavior having almost perfect reversibility [1,19].

Since the energetic and kinetics of bioprotein's stability and its decimation due to the adverse effects of the environment are becoming a central issue in these days, we have decided to present a robust irreversible thermodynamics formulation of the helical conformation relying on our recent mathematical solution of the unusual torsional deformation of a cylindrical bar having circular cross section, and its adaptation to the simple helical conformations [9]. Here, one more attempt has been made for the application of the irreversible non equilibrium theory as advocated by Ogurtani, [20] by taking into account the functional form of the unusual torque term explicitly, in terms of total pitch height along the direction of the cylindrical axis, while keeping the azimuthal angle of C-end of the amino-acid skeleton free to move. While doing that the amino acid skeleton is assumed to be enclosed by a cylindrical shell or the cage, which interacts with the immediate inner and outer aqua surroundings through the side branching molecular residues having characterized by the interfacial Gibbs specific free energy density for a isothermal closed system [9].

All those possible short range physico-chemical interactions (i.e., electrostatic dipole-dipole interactions), which might take place at the interfacial layer between the alpha-helical peptide and its immediate aqua environment can be describable in terms of the interfacial Gibbs free energy density function. Therefore, the global Gibbs free energy of the amino acid skeleton and its side branching, which combines the bulk and the surface Gibbs free energies of the isothermal closed system, uniquely determines the main features of the morphological evolution behavior of the alpha-helix in the space and time domain under the isothermal and isobaric conditions by introducing a proper reference system, which is the torsional and bending deformation free the straight line configuration of the "unfolded state".

Theory

The present mathematical formulation gives us great flexibility in using the irreversible thermodynamics connection [20] $d\nabla S_{in} / dt = -1/T d\nabla \tilde{G}/dt \geq 0$ between the rates of internal entropy production denoted by $d\nabla S_{in} / dt$ and the enlarged global Gibbs free energy change designated by $-1/T d\nabla \tilde{G}/dt$ as advocated by Ogurtani, [21,22] for the closed systems under the isothermal isobaric as well as isochoric conditions. In the last case, the global Gibbs free energy is replaced by the global Helmholtz free energy. Here, the closed system implies that the material content and the composition of the amino-acid back bone structure, and its side branches stay invariant. In this paper, we are proposing a concrete physical model to be used for the mathematical formulation of the aging thermokinetics of the amino-acid based bioprotein as a well-posed boundary value problem by starting from the alpha-helical conformation designated by 3.6_{13} as an initial state. However, the theoretical treatment is quite general can be applied any elastic body having simple helical conformations. We further assume that the amino-acid back-bone helical structure with its side wall branches and residues are enclosed by a cylindrical shell or cage with well-defined mean radius R and shell thickness h, which are invariant quantities similar to the total arc length l_o and radius of the amino-acid residues, a. Only the height of the cage, which is equal to the total pitch height p, and the total azimuthal angle θ of the helix that is determined by the free end of the helix are assumed to be quasi-free variables. These are connected by the constrain through the invariant arc length, and helical radius, respectively, l_o and R by the equation; $0 = p^2 + \Theta^2 R^2 - \ell_o^2$. This expression enters into the enlarged global Gibbs free energy function to be optimized, designated by $\nabla \tilde{G}(p, \Theta; \chi)$ as an additive term such as: $\nabla \tilde{G}(p, \Theta; \chi) = \nabla G(p, \Theta) + \chi(p^2 + \Theta^2 R^2 - \ell_o)$. Where χ is the Laplace multiplier [23], which acts as a parameter in collaboration with p and θ in the optimization procedures. Later, we will switch to the genuine global Gibbs free energy $\nabla \bar{G}(p)$ by eliminating theta azimuthal angle directly form the constrained mention previously, which would give us great flexibility to connect the variation in rate of internal entropy production under the isothermal conditions directly to the variation of the global Gibbs free energy change under the isothermal isobaric conditions.

Keeping all these complication in our mind, as a first step to handle this mesoscopic non equilibrium stationary state aging kinetics problem, we will rather employ a quasi-static approach by using a simple optimization procedure in connection with the enlarged version of Planck Criterion [24] by Ogurtani, which relies on the variational method [23] These free variations in $\delta \Delta \tilde{G}(p, \Theta, \chi)$ respectively, due to variations in the cage dimension δp and the azimuthal angle $\delta \Theta$, which produces a free end displacement of the amino acid chain that changes the inclination angle β of the helical conformation that reflects itself on the rotation $\lambda = Sin\beta Cos\beta / R$ and the curvature $\kappa = Sin^2\beta / R$ of the helix structure associated with the amino-acid skeleton. The variation in the global Gibbs free energy with respect to Θ and p while holding the constrain such as $\delta\{p^2 + \Theta^2 R^2 - \ell_o^2\} = 0$, may be represented by the following relationship corresponds to the specific surface Gibbs free energy denoted by g_s for the isobaric changes, which is represented by $PV = \pi R^2 pP$ term that can be replaced by $PV \Rightarrow \pi R^2 p \sigma$ in the case uniaxial tension or compression denoted by σk along z-axis of the helical conformation:

$$\delta \Delta \tilde{G} = \delta\left\{\frac{\pi}{3}Ga^2\lambda^2\ell_o^3 + 2\pi R g_s p + \pi R^2 p\, \mathrm{P} + \chi\left(p^2 + \Theta^2 R - \ell_o^2\right)\right\} = 0 \quad (1)$$

We may use the following connection for the torsion, which is also explicit function of $\{\Theta, p\}$ for the helical conformation, namely: $\lambda = R^{-1}\sin\beta\cos\beta \to R^{-1}(\Theta R / \ell_o)(p / \ell_o)$:

$$\delta\Delta G = \delta\left\{\frac{\pi}{3}Ga^2 p^2\Theta^2\ell_o^{-1} + 2\pi R g_s p + \pi R^2 pP + \chi\left(p^2 + \Theta^2 R^2 - \ell_o^2\right)\right\} = 0$$
$$(2)$$

Where Θ, p and χ are independent variables, and χ is the Lagrange multiplier[i]. The extremum problem may be obtained from the following two partial derivatives with respect to θ and p; namely:

$$\partial\Delta G / \partial p = 2\frac{\pi}{3}Ga^2 p\Theta^2\ell_o^{-1} + 2\pi R g_S + \pi R^2 P + 2\chi p = 0$$
and
$$\partial\Delta G / \partial\Theta = 2\frac{\pi}{3}Ga^2 p^2\Theta\ell_o^{-1} + 2\chi\,\Theta R^2 = 0 \quad (3)$$

One can eliminate χ terms from above two independent equations by multiplying the first line by $\Theta R^{2,}$ and the second line by p, and then applying subtraction operation to them, it follows:

$$2\frac{\pi}{3}Ga^2 p\,\Theta\left(\Theta^2 R^2 - p^2\right)\ell_O^{-1} + 2\pi\,\Theta R^3 g_S + \pi R^4\Theta P = 0 \quad (4)$$

This expression can be put into a very compact form by employing $0 = p^2 + \Theta^2 R^2 - \ell_o^2$, and then making some legitimate cancelations to produce the following form in Eq. (5)[ii].

$$p^3 - \frac{\ell_o^2}{2}p - \frac{3R^3\ell_o}{4a^2}\left(2\frac{g_S}{G} + R\frac{P}{G}\right) = 0 \quad (5)$$

[i] For the force-extension type mechanical test conditions, $\pi R^2 P$ corresponds to the applied force $\bar{F}$ along the z-axis of the fictitious cylindrical cage. If one uses the cylindrical shell model for the cage, then, $\pi R^2_p P$ should be replaced by, $2\pi Rh_p P$, where p is limited extension along the axis, h is shell thickness, which is thick enough to accommodate the amino acid backbone structure without the side branches and residues. That is about 1.5 A°. This reduces the effect of the applied pressure on the displacement velocity due to the reduction of the applied surface area by a factor of two in comparison with the interfacial Gibbs specific free energy density.

The expression on the left side saving a cofactor, it is actually corresponds to the negative of the gradient of the Global Gibbs free energy of the system with respect to the total pitch height. Therefore, it is nothing but the generalized force acting on the helical conformation under the prescribed constrains. The positive root of this equation denotes the position of extremum of the global Gibbs free energy with respect the total pitch height. The most critical parameters associated with the interfacial energy as well as the applied stresses, which play threshold levels or dividing boundaries are obtained from the solutions of this master equation. The second derivative of the global Gibbs free expression becomes zero (the inflection point) at the critical normalized total pitch height $\hat{p}_{cr} = p_{cr}/\ell_o = 1/\sqrt{6} \approx 0.40824$, which is a very important universal constant, and where the generalized force has a *minimum* regardless the values of the external parameters, such the applied pressures and the interfacial Gibbs free energy densities. The application of the critical pitch height in the normalized and scaled version of the above relationship Eq. (5), results a *threshold* value out of the combinations of the applied stresses and the interfacial free energies as shown in Eq. (6), which ensures that the generalized force is all along the path is positive definite. This threshold value also draws a trajectory that acts as a boundary line in $\{\hat{p}, \hat{t}\}$ space, between the non-equilibrium stationary states domain and the dynamic instability region, which are lying, respectively, at the upper and lower parts of the negative parametric manifold $\{g_s, P\}$.

$$\left(1/\sqrt{6}\right)^3 - \left(1/\sqrt{6}\right) = \frac{3R^3}{4a^2\ell_o^2}\left(2\frac{g_s}{G} + R\frac{P}{G}\right) < 0 \quad (6)$$

In order to get the irreversible thermokinetics behavior of the system, we have employed different strategy by starting from the genuine global Gibbs free energy relationship, which is given by Eq. (2) without the Lagrangian term, and then eliminate its azimuthal angle dependence using $\ell_o^2 = p^2 + \Theta^2 R_o^2$ connection associated with the helical conformation, that follows:

$$\delta\nabla G = \delta\left\{\frac{\pi}{3}\frac{Ga^2}{R^2}p^2\left(\ell_O^2 - p^2\right)\ell_O^{-1} + 2\pi Rg_Sp + \pi R^2 pP\right\},$$
and
$$\frac{d\Delta G}{dp}\delta p = \left\{\frac{\pi}{3}\frac{Ga^2}{R^2}\left(2p\ell_O - 4p^3\ell_O^{-1}\right) + 2\pi Rg_S + \pi R^2P\right\}\delta p \quad (7)$$

At this point we will introduce the connection between the rates of internal entropy production. which a positive definite quantity, and the rate of variation of the Global Gibbs free energy for the isothermal isobaric irreversible processes, or the natural processes [25]. Where the equal sign corresponds to the reversible or equilibrium processes.

$$\left.\frac{dS_{Int}}{dt}\right|_{T,P} = -\frac{1}{T}\left.\frac{\partial\Delta G}{\partial p}\right|_{T,P}\frac{dp}{dt} \geq 0 \quad (8)$$

The right hand side can be decomposed into the generalized force and the conjugate flux [26]:

$$\frac{dp}{dt} = -\frac{\mu}{kT}\left\{\frac{\pi}{3}\frac{Ga^2\ell_o^2}{R^2}\left(2p/\ell_o - 4(p/\ell_o)^3\right) + 2\pi Rg_S + \pi R^2P\right\} \quad (9)$$

Where, μ is generalized mobility as defined by Onsager Theory [26]. Then, the conjugated flux and the generalized global force, which are associated with the production of entropy per unit time may be designated, respectively, as $F_G = -\frac{1}{T}\left.\frac{\partial\Delta G}{\partial p}\right|_{T,P}$ and dp/dt. The force term may be put into the following format after some normalization procedures, which will be used later in the graphical representations:

$$F_G = -\frac{1}{T}\frac{4\pi Ga^2\ell_o^2}{3R^2}\left\{\left(\frac{1}{2}p/\ell_O - (p/\ell_O)^3\right) + \frac{3R^3}{4Ga^2\ell_O^2}(2g_S + RP)\right\} \quad (10)$$

Application of the same normalization procedure to Eq. (9), the following expression denoted as Eq. (11) may be obtained for the displacement speed of the height of the helical conformation, which takes place by allowing C-end of the peptide to glide along the z-direction at the surface of the hypothetical cylinder or "cage".

$$\frac{d(p/\ell_o)}{dt} = -\left(\frac{\mu}{kT}\frac{4\pi}{3}\frac{Ga^2\ell_o}{R^2}\right)\left\{-(p/\ell_o)^3 + \frac{1}{2}(p/\ell_o) + \frac{3}{4}\frac{R^3}{a^2\ell_o^2}\left(\frac{2g_s}{G} + R\frac{P}{G}\right)\right\} \quad (11)$$

One can immediately anticipate from the above given explicit format that the relaxation time of the irreversible process of unfolding is $\tau = \left[\frac{\mu}{kT}\frac{4\pi}{3}\frac{Ga^2\ell_o}{R^2}\right]^{-1}$ sec., and where μ [cm²/sec.] is the generalize mobility appears in the Onsager's [26] relationships between the generalized forces and conjugated fluxes [iii]. Here, the mobility μ may be represented by an Arrhenius relationship such as $\mu = \mu_O \exp(-Q/kT)$, where μ_0 is the mobility constant, which is temperature independent, and it involves Debye vibration frequency and the entropy of activation as a steric factor.

The second term in Eq. (11) between the braces on left side is nothing but the gradient of the Global Gibbs free energy of the system, and the minus of which is the generalized force. The connection here is done by the generalized mobility, which looks very similar to the Nernst-Einstein mobility 'saving the steric factor' [7] used in dissipative convection problems, or the transport problems driven by external agents. This relation may be further normalized and scaled, respectively, by taking following dimensionless quantities. $\hat{p} = p/\ell_o$ and $\hat{t} = t/\tau$.

$$\frac{d(\hat{p})}{d\hat{t}} = -\left\{-\hat{p}^3 + \frac{1}{2}\hat{p} + \frac{3}{4}\frac{R^3}{a^2\ell_o^2}\left(\frac{2g_s}{G} + R\frac{P}{G}\right)\right\} \quad (12)$$

For the shake of demonstrations, the following numerical solutions under the various applied pressures are presented in graphical format: In figure 1a, each plot up to -1.057 GPa pressure, has a negative displacement velocity sector, which has its own upper limit, which is determined from the positive root

of the second derivative of the Global Gibbs free energy that is a universal constant given by $\hat{p}_{cr} \equiv (\hat{p}/\ell_o) = 1/\sqrt{6}$. This number can be used in equation Eq. (5) to get Eq. (6), which produces, respectively, the desired value for the applied pressure [-1.057 GPa], and/or the interfacial specific Gibbs free energy [g_s=-317 erg/cm^2]. This threshold level constitutes an upper bond for a sub-region in the negative domain of the $\{\hat{p}, \hat{t}\}$ plane, which is bounded by the zero applied pressure curve at the bottom of the negative manifold, in which alpha-polypeptide may evolve towards the stationary nonequilibrium states either contracting or extending depending upon whether it is below and above the singularity. This singularity takes place when the upper limit of the integral in Eq. (15) becomes equal to the lower limit, respectively. The corresponding hydrostatic stress or the interfacial free energy may be obtained from Eq. (5) by substituting $\hat{p}_o \Leftarrow p_o/\ell_o$, which is 1.4 for the alpha-helix designated by 3.6_{13}. The generalized force for the various values of the applied stresses is illustrated in figure 1a for further discussions. As mentioned previously all these curves have the same minimum at $\hat{p} = 1/\sqrt{6}$, and there is also a vertical dashed-line drawn at $\hat{p} = 1/\sqrt{2}$, which corresponds to the maximum torsional elastic energy stored in the helical conformation.

In figure 1b, the plots are extended beyond the unfolding range to see the behavior of the force extension connections. Where, a new red line [5GPa] is added. Otherwise, all other four lines look like to be superimposed into a single universal line represented by the first two terms in Eq. (10). Actually that is not the case! This only shows that the effect of the hydrostatic pressure up to 500 MPa is negligible.

Our extensive computer simulation has showed that the first two terms, which come directly from the stored elastic energy in Eq. (8) are very imported in spontaneous unfolding process not only for the isobaric case but also for the isochoric conditions, where no externally applied traction and body forces are exist. To get some panoramic picture of its contribution to the overall relaxation process, one may put that part into the analytic format for the further integration procedure: namely;
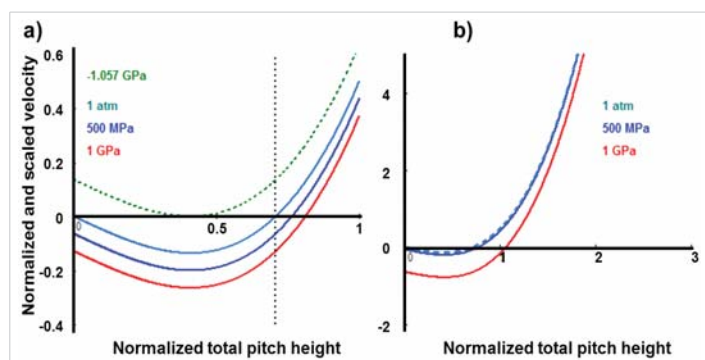
Figure 1: a) Displacement velocity of the total pitch height is presented for the various applied hydrostatic pressures or the equivalent uniaxial compression and tension stresses. b) a new red line added, which belongs to the interfacial free energy of 5GPa. Otherwise, all other four lines look like to superimpose into a single universal line represented by the first two terms in that equation but it is not!

$$\int_0^{t/\tau} d/(t/\tau) = -\int_{po/\ell_o}^{p/\ell_o} \frac{d(p/\ell_o)}{(p/\ell_o)\left\{\frac{1}{2}-(p/\ell_o)^2\right\}} = -\ln\left(\left(\frac{p/\ell_o}{po/\ell_o}\right)^2 \frac{1-2(po/\ell_o)^2}{1-2(p/\ell_o)^2}\right) \quad (13)$$

This can be written as a normalized and scaled form, respectively, to the relaxation time, τ and contour length ℓ_o of the alpha polypeptide, as follows:

$$\bar{t}(\hat{p}, \hat{p}_o) = -\ln\left(\left(\frac{\hat{p}}{\hat{p}_o}\right)^2 \frac{1-2(\hat{p}_o)^2}{1-2(\hat{p})^2}\right) \quad isochoric\ isolation \quad (14)$$

In the case of multi- helical conformations having loosely connected by horizontal strands such as DNA, which has a double helix configuration, the form of this functional relationship wouldn't change but only the effective relaxation time of the network should be calculated as: $\bar{\tau}^{-1} = \sum_k \tau_k^{-1}$. The time versus total pitch height relationship given by Eq. (13) can be inverted using some legitimate arithmetic operations.

Then one may follow up the time variation of the unfolding process during the aging directly, to get some sound reflections about the aging behavior of this spontaneous isothermal unfolding process at the absence of outer interferences:

$$p/\ell_o = \frac{(p_o/\ell_o)\exp(-t/2\tau)}{\left\{1-2(p_o/\ell_o)^2\left[1-\exp(-t/\tau)\right]\right\}^{1/2}} \quad (15)$$

In figure 2a, the morphological evolution behavior of the alpha peptide exposed to an acidic environment, which is represented by a negative interfacial specific Gibbs free equivalent to the threshold level of [g_s=-317 erg/cm^2] is demonstrated. Here, the unabridged scaled relationship Eq. (16) is employed for the numerical computations, which is deduced by applying a formal integration procedure to the connection denoted by Eq. (11) after some rearrangements of terms for the normalization. At the nonequilibrium stationary state regime, this trajectory shows 185% extension, which amounts to 3.02 nm change in the total pitch height compared to the initial total pitch height of 1.62 nm [iv].Actually this corresponds to the maximum attainable total normalized pitch height of $\hat{p} = 1/\sqrt{6}$; 0.40, which can be reached at the nonequilibrium stationary state regime, regardless the initial state described by $\hat{p}_o = p_o/\ell_o$. However, this configuration is extremely unstable with respect to the fluctuations in the external parameters as will be demonstrated later in section.

In figure 2b, the universal aging function represented by Eq. (15) is introduced with respect to the normalized time on the semi-logarithmic plot, which shows a typical S-shape curve by approaching asymptotically to the zero value. This function may be used for the determination of the life time expectations of alpha-polypeptides or bioprotein having helical conformation including the rather complex multi-helical conformations such as DNA by just adjusting the relaxation time of the system using the network theory as described in the **Appendix.** Where, the interactions

---

[iv] Initial, and final global Gibbs free energies are, respectively, E_o = -9.063 eV/molecule, and E_F = -13.203 eV/molecule. **b:** In the second case, the relaxation of the rotational elastic energy of Alpha Helix takes place from E_o =3.03 eV/molecule, down to E_F= 0.027 eV/molecule. Here, only the bending elastic energy is left, which is about $E_b \cong 7.507 \times 10^{-3}$ eV /molecule. Where the initial value is $(p_o/\ell_o) = 0.1396$, which corresponds; $p_o = 16.2 A^o$ and $\ell_o = 116 A^2$.
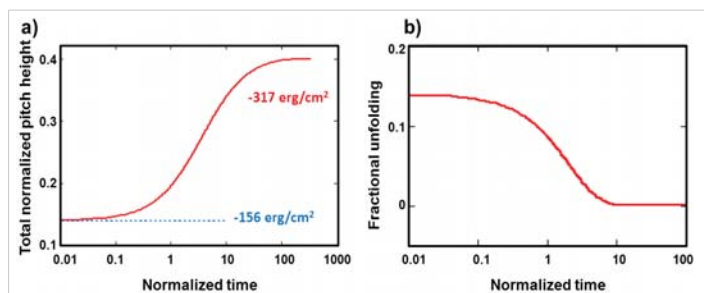
Figure 2: a) The unfolding of a Helical conformation 3.6_{11} with expansion in the stability region of the negative hydrostatic pressure and interfacial free energy manifold driven by the stored elastic torsional energy in collaboration with the critical interfacial Gibbs free energy. b) Isochoric unfolding at absence of the surface and hydrostatic pressure terms. It is solely driven by the stored torsional elastic energy, which is about 3 eV/molecule.

between the side wall branches and the inner horizontal strands with the immediate surroundings are considered in the interfacial specific Gibbs free energy "volumetric" densities [27] associated with the inner and outer "surface layers" of the cylindrical shell or the cage enclosing the both amino acid skeletons of the duplex-helical conformations of DNA [28].

In figure 3, Global Gibbs free energy for the helical alpha peptide is presented as a function of the total pitch height for the various values of the hydrostatic pressure. Numerical experiments, which will be presented in the next section, show that as long as the initial total pitch height of the helical conformation satisfies the connection of $\hat{p}_o \leq 1/\sqrt{2} \approx 0.707$, the isobaric and the isochoric systems spontaneous unfold towards the flat configuration if the constant term in Eq. (10) is positive definite and zero, respectively. That means, the sum-over the interfacial energy (isochoric only) and the applied hydrostatic pressure dominantly should be non-negative; $(2g_s + RP) \geq 0$. The effect of this constant term on the thermo-kinetics of the unfolding of the alpha-helix becomes clear when we integrate that unabridged equation. Similarly to get the full effect of the physico-chemical terms in Eq. (12), it will be put into the following integration format, which involves only the normalized variables and dimensionless constant. Unfortunately this integral doesn't have any close form solution even though it looks very simple.

$$\left.\frac{t}{\tau}\right|_{t_o}^{t} = -\int_{po/\ell_o}^{p/\ell_o \leq 1} \frac{dx}{\left\{ x\left(\frac{1}{2} - x^2\right) + \frac{3R^3}{4a^2\ell_o} \times \left(\frac{2g_s}{\ell_o G} + \frac{R\,P}{\ell_o G}\right) \right\}} \qquad \text{where } x \equiv p/\ell_o \leq 1 \quad (16)$$

This constant term involves two external tunable parameters normalize with respect to the shear modulus of the amino-acid back bone structure, namely; the interfacial specific Gibbs free energy, $(g_s/\ell_o G)$ and the applied hydrostatic pressure $(g_s/\ell_o G)$, which equally well may be used for the uniaxial tension or the compression to simulate the mechanical test conditions. In this formulation, to avoid unnecessary complications, we have considered only outer wall of the shell, which is composed of molecular residues attached to the "amino-acid skeleton", and are interacting strongly with its immediate environment through the multi-pole electrostatic force field [29].
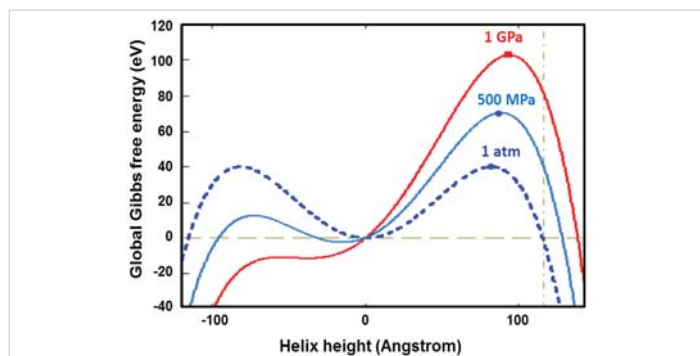
Figure 3: Global Gibbs free energy of α-Helix 3.6_{13} is plotted with respect to the total pitch height For various values of the applied stress in absence of the interfacial Gibbs free energy. Eq. (10) operates only in domain, where $\ell_o \geq p \geq 0$, the rest is given for the illustration. One would have very similar plots for the positive interfacial free energies. The negative gradients of these curves give the directions of the natural time evolutions of helical conformation.

In that stationary nonequilibrium state having flat configuration, there is only bending energy left to be considered, which is given by $E_b = 1/2 E_Y \kappa^2 \left(\pi a^4/4\right)$ according to Ogurtani [9] for the helical confirmation. Where, $E_Y \rightarrow 3G$ is the Young modulus assuming that Poisson's ratio is $\upsilon = 0.5$, and κ is the curvature that is given by $\kappa = R^{-1}\sin^2 \beta \Rightarrow R^{-1}$, and for the flat configuration $\beta = \pi/2$. The close inspection of the torsion formula for the simple helix, which can be put into the following format by its definition [30] $\lambda = \sin 2\beta / 2R$. This expression shows that the torsion takes extremum value $\lambda_{ex} = 1/2R$ for the odd integer multiplies of $\pi/4$, namely; $\beta_{ext} = (2n+1)\pi/4$. On the other hand the rotational energy is proportional with λ^2, which means that these extremal values correspond to the maximum elastic energy, which corresponds to the real roots in the variational problems.

Results and discussions

The results of the computer experiments done on the enlarged formulation of the unfolding and stability of helical conformation are introduced in this section in graphical formats. These are obtained by employing large set of internal and external parameters in the numerical solution of the scaled and normalized thermokinetics evolution equation given by Eq. (17)[v], which has an exact analytical solution at absence of the constant term as demonstrated in previous section. That solution acts as a dividing line between the positive and negative hydrostatic pressures and interfacial Gibbs specific free energies manifolds, which play the major role in the life time of the alpha-polypeptides whether they can survive or decimate.

$$\left.\frac{t}{\tau}\right|_{t_o}^{t} = -\int_{po/\ell_o}^{p/\ell_o \leq 1} \frac{dx}{\left\{ x\left(\frac{1}{2} - x^2\right) + \frac{3R^3}{4a^2\ell_o^2} \times \left(\frac{2g_s}{G} + R\frac{P}{G}\right) \right\}} \qquad \text{where } x \equiv p/\ell_o \leq 1 \quad (17)$$

This is an evolution type of integral equation that represents a highly nonlinear dynamic system, and the functional behavior

of which strongly dependents on, where the initial total pitch height of the helical conformation (designated as the lower limit of $\hat{p}_o = p_o / \ell_0$ for integration procedure) lies with respect to the critical value of the total pitch height denoted as $\hat{p}_{cr} \equiv (p_{cr} / \ell_0) = 1/\sqrt{2}$. Where the inclination angle of the helical conformation becomes $\beta_{max} = 45°$. This critical angle corresponds to not only the maximum rate of change in the twist angle along the ach length described by $\lambda_{max} = Sin 2\beta_{max} / 2R \rightarrow 1/2R$, but also the maximum torsional elastic energy can be stored in the any simple helical configuration [9,31].

In figure 4, the various manifolds and regions are represented by the total pitch velocity versus normalized pitch height connections obtained from Eq. (12) using some critical interfacial specific Gibbs free energy densities introduced in the previous section. There are the green and turquois lines, which enclose the stationary state region. Above the green line denoted as g_s = 317 erg/cm² lays down a region, where the displacement velocity is positive definite and the helical conformation exposed to an extension, having well definite asymptotic limit of $\hat{p} \rightarrow 0.388$. The region below the turquois line denoted by $g_0 = 0$, belongs to the positive manifold, which shows negative displacement velocities in the interval of [$0 < \hat{p} \leq 0.14$], which spans the complete unfolding range for the alpha-peptide. That is region, where the aging or unfolding takes place with the rate, which increases with the increase in the interfacial free energy density or the hydrostatic pressure.

In figure 5, the normalized times required for the alpha-peptide 3.6_{13} to reach for the prescribed total pitch heights are calculated from Eq. (17) for various positive and negative values of the interfacial Gibbs specific free energies, and then presented in terms of the trajectories in space and time domain. This figure shows that up to the critical interfacial free energy density denoted as g_s =-156 erg/cm², the unfolding in the negative manifold below that line takes place with "shrinkage", while the alpha peptide is gradually approaching to one of those nonequilibrium stationary states. On the other hand, the transitions towards stationary states in the upper interval [-156 $\leq g_s \leq$ -317] take place by extensions in the initial total pitch height of alpha helix. The most interesting feature of this sub-region is that it is divided into two sectors by a straight line designated by $\hat{p} = \hat{p}_o = 0.14$, and that corresponds to -156 erg/cm², which may be deduced directly from Eq. (5) by letting $p / \ell_o = 0.14$.

In figure 6, the critical initial configuration of a helical peptide occurs when the initial normalized total pitch height is $1/\sqrt{2}$, which corresponds to the maximum stored torsional elastic energy of 40 eV/molecule. One consequence of this high energy is the sharp division of the positive and negative manifolds, and the complete missing of the nonequilibrium stationary state regime regardless its secondary features. The positive manifold ends up with the typical aging behavior, which ends up with the collapsed flat rings configuration having zero torsional elastic energy. The remaining bending energy is about 7.507 x 10⁻³ eV/Molecule, which is extremely small compared to the initial stored energy of helix that is about + 40 eV/molecule. Any helical conformation at the negative manifold, where $g_s < 0$ or $p < 0$ ends up with the
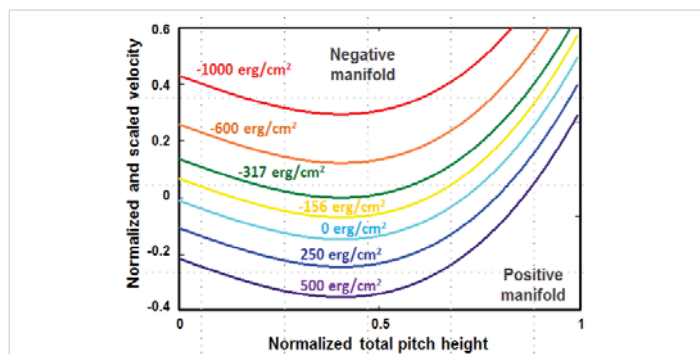
Figure 4: The scaled pitch velocity versus total pitch height is plotted with respect to the selected values of the interfacial Gibbs specific free energy to show those two distinct manifolds separated by the velocity sign inversion line.
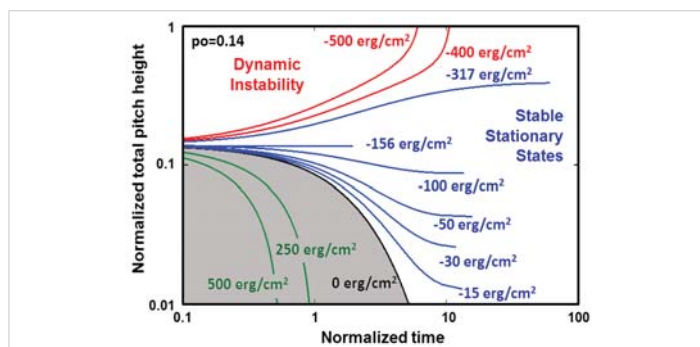
Figure 5: The unfolding of Helical conformation of α- peptide designated as 3.6_{11} is illustrated for various values of the positive and negative hydrostatic pressure at absence of the interfacial Gibbs free energy using Eq. (13).
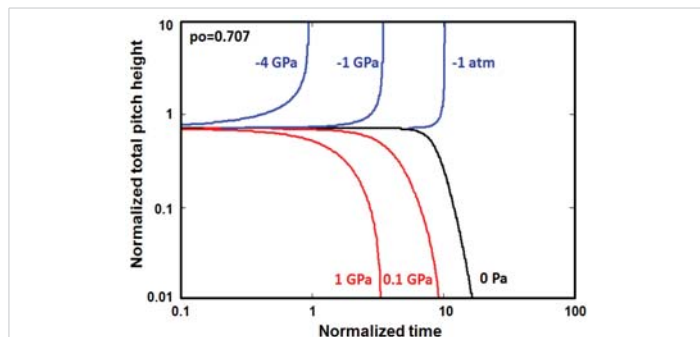
Figure 6: The unfolding of a Helical conformation, which has a critical total pitch as an initial configuration $p_O / \ell_O = 1/\sqrt{2}$ under the action of the various positive and negative hydrostatic pressures. This initial pitch height corresponds to the maximum elastic torsional energy, where the inclination angle for the torsion becomes: β = 45°. Threshold level, which separates the stability and dynamic instability manifolds is $p = 0$ or g_s = 0erg/cm².

straight vertical line configuration having zero stored torsional and bending elastic energies. However, the global Gibbs free energy reaches to a value of -82 eV/molecule at the end of the full unfolding. That means the total energy injected to the system by the applied negative pressure or the work done by the applied uniaxial tension is about 122 eV/molecule. This figure is much closed to the unfolding energy of 1000 kJ/mol. [104 eV/molecule], which is obtained by Idiris, et al. [2], from the stretching experiments on a single (Glu)$_n$ Cys at the acidity level of 3pH by assuming that the initial length of helical conformation is about 10 nm and extending up to 25 nm at 3.0 pH acidic environment [See: their histogram in figure 5].

In figure 7, the morphological evolution of alpha-helix having initial pitch height, $\hat{p}_o = 0.5$, just below the critical value, where the initial elastic stored energy is $E = 29.9$ eV/molecule, which is not strong enough to push the helical conformation to the upper dynamic instability regime, without the help of the large negative interfacial free energy or the uniaxial tension but rather to proceeds towards the nonequilibrium stationary states below the threshold level of -973.4 MPa or [g_s = -292.014 erg/cm^2] with the decrease in the total pitch height. The threshold level may be calculated from Eq. 5 by inserting $p / \ell_o = 0.5$. It is also clear from figure 7 that there is an about one order of magnitude enhancement in the relaxation life time at the lower edge of the threshold level, while taking place about 30% reduction in the pitch height if the system is exposed to the proper uni-axial tension and/or the negative interfacial free energy.

Figure 8 shows very unusual behavior of the morphological evolution of helical conformation, which has an initial total pitch height well above the critical total pitch height $\hat{p}_o = 0.80 > 1/\sqrt{2}$ that is introduced in the previously. The stored elastic torsional energy initially is about 36.8 eV/molecule, which is high enough to push the system into the dynamic instability region even with the positive hydrostatic pressure up to +870 MPa. [or $g_s = 255$ erg/cm^2]. Above this level namely at 895GPa [or $g_s = 269$ erg/cm^2], the unfolding process switches back to the aging regime without showing any existence of the nonequilibrium stationary states, and rather asymptotically approaches to the flat configuration, showing a similar trend given in figure 2b. For this initial total pitch height, the threshold level is calculated from Eq. 5, and it is found to be [872.1MPa] and $g_s = 261.44$erg/cm^2. Similarly, the alpha- helix even at the absence of the external interventions (green dotted line) can't relax towards the stationary state flat configuration but rather forced to go to the opposite direction ever increasing in velocity, finally to end up with the large extension on its amino acid back bone skeleton or the cord length, which may end up in catastrophic decimation.

In figure 9, a snap-shut is presented from the alpha-peptide 3.6_{13} while it is evolving in an environment as such that its influence on the system is characterized by an interfacial Gibbs specific free energy of $g_s = + 500$ erg/cm^2 [is equivalent of 1.667 GPa hydrostatic pressure]. The initial stored torsional elastic energy is 2.959 eV/molecule, which drops down to 0.08 eV/molecule. The initial state (red dotted line) is described by $\hat{p}_o = 0.14$, which corresponds to the total pitch height of 5.4 x 3 = 16.2 A^o, and the arc length 116 A^o. That is exactly equivalent to the alpha-peptide DNA 3.6_{13} as investigated and reported by Pauling–Corey–Branson [11]. This snap-shut is selected at the point of $\hat{p} = 0.01$ on the total pitch height versus time plot in figure 5, that amounts to a flight time of $t = 0.52$ τ sec., where τ is the relaxation time of the unfolding process is defined previously.

The Global Gibbs free energy of the alpha helix for this snap shut position is 1.38 eV/molecule compared to its still remained torsional elastic energy, which is about 0.06 eV/molecule. This difference comes from the interfacial Gibbs free energy between

J . < / g i v e n - n a m e s >
</name>
</person-group>
<article-title>Artificial intelligence in radiology: who’s afraid of the big bad wolf</article-title>
<source>
<italic toggle="yes">European Radiology</italic>
</source>
<year>2019</year>
<volume>29</volume>
<issue>4</issue>
<fpage>1637</fpage>
<lpage>1639</lpage>
<pub-id pub-id-type="doi">10.1007/s00330-018-5995-9</pub-id>
<pub-id pub-id-type="other">2-s2.0-85061234177</pub-id>
<pub-id pub-id-type="pmid">30734848</pub-id>
</element-citation>
</ref>
<ref id="B252">
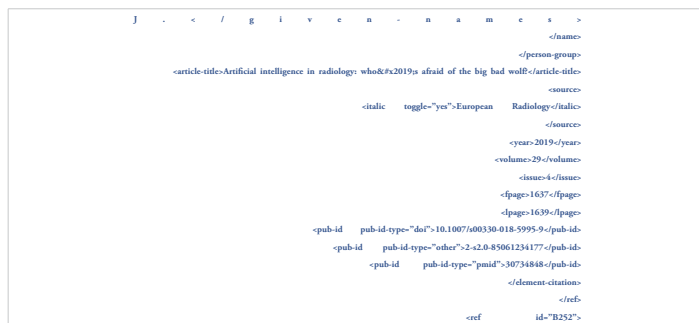
Figure 7: The unfolding of a Helical conformations, which have total pitch heights $p_o / \ell_o \Rightarrow 0.50$ below the critical value of $p_{cr} = \ell_0 / \sqrt{2}$ as an initial configurations under the action of the various positive and negative hydrostatic pressures. Threshold level is - 973.4 MPa [g_s= -292.014 erg/cm^2] may be calculated from Eq. 5 by letting $p = p_o$. This initial configuration shows the nonequilibrium stationary states regime below the threshold level up the boundary of the aging region marked by dotted red line.
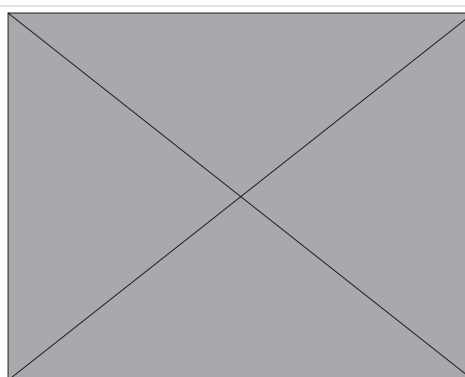
Figure 8: The unfolding of a Helical conformation, which has an initial pitch height $p_o / \ell_o \Rightarrow 0.80$, above the critical value of $\hat{p}_o > 1/\sqrt{2}$, shows two distinct regions under the hydrostatic pressure separated by a threshold level. Above which it is completely in the state of instability, which is ending up with the complete unfolding with zero elastic rotation and bending energies. The other region shows stability with decreasing in pitch height up to the flat configuration. The hydrostatic pressure in this regime decreases the relaxation life time in the stability domain. This just the opposite in the case of dynamic instability regime, where it increases. Threshold level is 872.1 MPa [g_s = 261.014 erg/cm^2] may be calculated from Eq. 5.
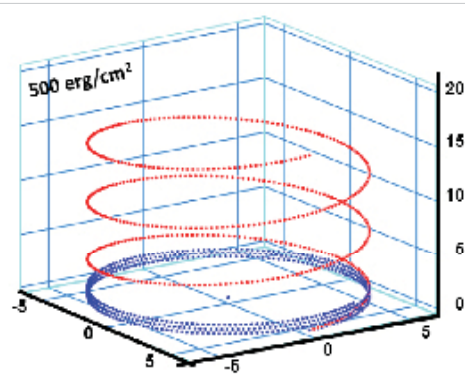
Figure 9: Helical conformation of α - peptide at the stationary state is illustrated by (red dotted line), which has pitch height 5.4A^o, and radius 6A^o and 3 rings. When it is exposed to the spontaneous relaxation under the positive interfacial Gibbs free energy of g_s = +500 erg/cm^2 [= 1.677GPa] under 1 ATM pressure (isobaric) then the unfolding takes place (blue line), which is found to be 86.4% of the full transition, having Θ = 3.077 cycle.

alpha peptide and its surrounding. At the start the Global Gibbs free energy is calculated and found to be + 22.14 eV/molecule due to large contribution coming from the interfacial free energy compared to the stored elastic energy of 2.959 eV/molecule.

Actually, still there is a drastic drop in the Global Gibbs free energy as well as in the stored elastic energy of the alpha peptide during the aging process. This is a typical dissipative irreversible process as one expects a priory. The close inspection shows that the number of turn around the z-axis is extended such as $\Theta/2\pi$ = 3.077 cycle instead of three that is the case for the folded state.

In figure 10, we take another extreme case relying on the map introduced in figure 5 by taking a trajectory for the alpha-peptide 3.6_{13}, which is characterized by an interfacial Gibbs specific free energy of g_s = 500 erg/cm² [is equivalent of 1.667 GPa uniaxial tension] that is enough to push the system into the dynamics instability regime. The snap-shut is taken at a point, which is very close to the completion of the unfolding process that is evolving along the path described in the space and time domain designated as the dynamic instability manifold in figure 5. The initial folded state has exactly the same configuration of the alpha-peptide designated as 3.6_{13}, which was investigated and reported by Pauling–Corey–Branson [11]. This snap-shut is selected at the point of $\hat{p}$ = 0.999 on the total normalized pitch height versus time plot in figure 5, that amounts to a flight or life time of t = 0.62 τ sec, where τ is the previously defined relaxation time of alpha-peptides. The Global Gibbs free energy of the alpha helix is calculated from the more transparent formula given by Eq. (6), and it is found to be -136.67 eV/molecule due to the contribution coming from the interfacial interaction with the surroundings. On the other hand, still some part of the stored torsional elastic energy remained in the helical conformation because of the incomplete unfolding, which is about + 0.318 eV/molecule that is much less than the initial stored elastic energy of + 2.959 eV/molecule. Actually if one takes a snap-shut at $\hat{p}$ = 0.999 the elastic rotational energy drops down to 0.032 eV/molecule, and it becomes exactly equal to zero when $\hat{p} \Rightarrow \ell_o$. However, this extreme case is not preferred to be used here for the demonstration purpose. This large dissipative energy difference between the present and the previous cases comes from the fact that there is large activation

energy barrier at $\hat{p} = 1/\sqrt{2} \rightarrow 83 A^o$ that has to be surmounted by the alpha-peptide in order to reach the final unfolding configuration by stretching, which has a straight line form having zero torsional as well as the bending energies, because of $\beta = 0 \Rightarrow \{\kappa = 0; \lambda = 0\}$.

Conclusion

A through numerical simulation has been performed to reveal the fine details of the morphological evolution behavior, and the aging kinetics of the -peptide or DNA in regards to the nonequilibrium stationary state regimes as well as dynamic instabilities, under the applied stress systems (ASS) while trying to take into account the strong multipolar electrostatic interactions at the interface. These interactions between the side-wall molecular branches and their immediate surroundings have been put into the sound numerical bases, not only by introducing the concept of interfacial specific Gibbs free energy densities (IGFE) but also assigned them a wide landscape of the negative and positive real number manifolds.

1. The first manifold: covers the whole positive values of the hydrostatic pressure "uniaxial compression" and the interfacial Gibbs specific free energy density landscapes, in which the helical conformation of alpha-polypeptides "amino acid skeleton, DNA" shows a typical aging behavior by shrinkage while approaching asymptotically towards the stationary non-equilibrium states having a flat circular configuration without any torsional elastic energy that may be called "quasi-extinction". This aging scenario indicates a steady decrease in the expectation value of the life time if one would increase the applied positive hydrostatic pressure and/or the positive interfacial specific Gibbs free energy density. But the effect of the hydrostatic pressure up to 100 Atm (1000 m depth in seawater) on the life time of α-peptide 3.6_{13} is almost negligible. That may be comparable with the similar aging effects caused by presence of the positive interfacial Gibbs free energy densities in the range of g_s = 3-4 erg/cm² for alpha-peptide 3.6_{13} conformation. Therefore, one should be very careful in evaluating the adverse effect of the pH level of aqua environmental pollutions on the interfacial Gibbs free energies compared to the effects of its co-partner, which is the positive hydrostatic pressure. Especially, if one deals with the aging behavior of habitats as well as the microorganisms, respectively, are living in the deep and shallow seawaters.

2. The second manifold: which covers the whole negative hydrostatic pressures "thermal expansion and/or uniaxial tension", as well as the negative interfacial specific Gibbs free energy spectrum mostly associated with the acidic environments (3-4 pH). The second manifold has a lower boundary line, which is the upper bond of the positive manifold mentioned above, and it is described by Eq. 15. This is a highly complex manifold compared with the previous one, which contains two subsets. Namely the lower subsets, where the nonequilibrium stationary state regime can be realized with and without the shrinkage in the total pitch heights. This subset is also divided into two sectors by a straight line designated by $\hat{p}_o$ = 0.14, which corresponds to the interfacial Gibbs free energy about g_s = -156 erg/cm² or equivalent to the
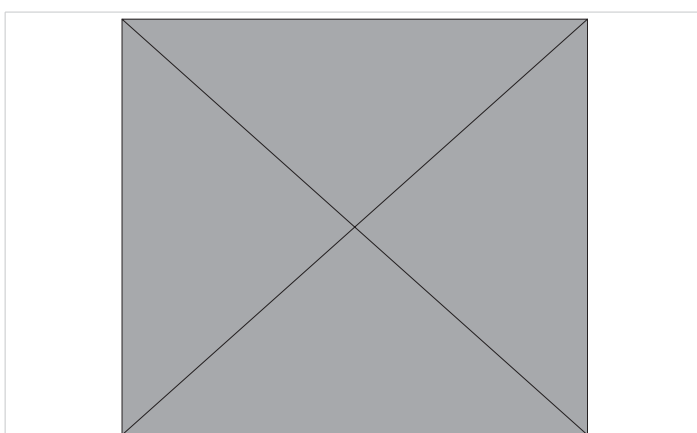
Figure 10: a) Perspective view: Helical conformation of α - peptide at the stationary state is illustrated by (red dotted line), which has pitch height 5.4Aᵒ, and radius 6Aᵒ and 3 rings. When it is exposed to the spontaneous relaxation under the negative interfacial Gibbs free energy of g_s = -500 erg/cm² [p = -1.677GPa uniaxial tension, isobaric] the unfolding takes place (blue line), which is found to be 99.9% of the full transition b) Top View: Partial unfolding appears as an arc segment (blue color) having Θ = 49.5ᵒ azimuthal angle with a torsional inclination angle of β = 2.563ᵒ. That should be zero if one takes final total pitch height as p = ℓ_o.

applied uniaxial tension of p = -0.528 GPa in the case of alpha peptide 3.6_{13}. The division boundary between the upper and the lower regions of the second manifold can be uniquely determined in terms the free energy and/or the stress or even with their linear combinations. The trajectory of the diving path involves a interfacial free energy of g_s =-317 erg/cm², or equally well with a constant applied uniaxial tension of p = -1.057 GPa, in the case of alpha peptide 3.6_{13}. That threshold can be obtained by inserting $\hat{p} = 1/\sqrt{6}$ into the master relationship denoted by Eq. 5. Idiris, et al. [1], are claiming that the acidity in the range of 3-4 PH of the embedding aqueous solution strengthening the helical conformation by increasing its unfolding energy and force, and the slightly basic and/or neutral environment just opposite they inhibits helical formation but rather enhanced crossed coil states [32].

Acknowledgment

References

1. Idiris A, Taufiq M, Ikai A. Spring mechanics of α–helical polypeptide. Protein Eng. 2000; 13: 763-770.
   PubMed: https://www.ncbi.nlm.nih.gov/pubmed/11161107

2. Misères A, Guenette PA. Phase transition-induced elasticity of alpha-helical bioelastometric fibers and networks. Chem Soc Rev. 2013; 42: 1973-1995.
   PubMed: https://www.ncbi.nlm.nih.gov/pubmed/23229440

3. Ackbarow T, Chen X, Sinan K, Buehler MJ. Hierarchies, multiple energy barriers, and robustness govern the fracture mechanics of α-helical and β-sheet protein domains. Proc Natl Acad Sci U S A. 2007; 104: 16419-16415.
   PubMed: https://www.ncbi.nlm.nih.gov/pubmed/17925444

4. Carrion-Vazquez M, Oberhauser AF, Fisher TE, Marszalek PE, Li H, et al. Mechanical design of proteins studied by single-molecule force spectroscopy and protein engineering. Prog Biophys Mol Biol. 2000; 74: 63-91.
   PubMed: https://www.ncbi.nlm.nih.gov/pubmed/11106807

5. Rief M, Pascual J, Saraste M, Gaub HE. Single molecular force spectroscopy of spectrin repeats: Low unfolding forces in helix bundles. J Mol Biol. 1999; 286: 553-561.
   PubMed: https://www.ncbi.nlm.nih.gov/pubmed/9973570

6. Bell GI. Model for the specific adhesion of cells to cells. Science. 1978; 200: 684-293.
   PubMed: https://www.ncbi.nlm.nih.gov/pubmed/347575

7. Yeremin EN. The Foundations of Chemical Kinetics. MIR Publishers-Moscow. 1976; 214-241.

8. Christian JW. The theory of transformations in metals and alloys, CH-3. Pergamum Press Oxford. 1975; 77-104.

9. Ogurtani TO. Enlarged version includes variational optimization of the length and Helmholtz binding free energy of α-helix: Curvature, Torsion and Torque in Helical Conformations and the Stability and Growth of alpha-Peptides under the Isochoric and Isobaric Conditions.

10. Kitano H. Computational system biology. Nature. 2002; 420: 206-210.

11. Pauling L, Corey RB, Branson HR. The structure of proteins: Two hydrogen bonded helical configuration of polypeptide chain, Proc Natl Acad Sci U S A. 1951; 37: 205-211.
    PubMed: https://www.ncbi.nlm.nih.gov/pubmed/14816373

12. Smeller L. Pressure-temperature phase diagrams of biomolecules. Biochim Biophys Acta. 2002; 1595: 11-29.
    PubMed: https://www.ncbi.nlm.nih.gov/pubmed/11983384

13. Kojima H, Ishijima A, Yanagida T. Direct measurement of stiffness of single actin filaments with and without tropomyosin by in vitro nanomanipulation. Proc Natl Acad Sci U S A. 1994; 91: 12962-12966.
    PubMed: https://www.ncbi.nlm.nih.gov/pubmed/7809155

14. Radmacher M, Fritz M, Cleveland JP, Walters DR, Hansman PK. Imaging adhesion forces and elasticity of lysozyme adsorbed on mica by atomic force microscopy. Langmuir. 1994; 10: 3809-3814.

15. Afin R, Alam MT, Ikai A. Pretransition and progressive softening of bovine carbonic anhydrase II as probed by single molecule atomic force microscopy. Protein Sci. 2005; 14: 1447-1457.
    PubMed: https://www.ncbi.nlm.nih.gov/pubmed/15929995

16. Afin R, Takahashi I, Shiga K, Ikai A. Tensile mechanics of alanine-based helical polypeptide: Force spectroscopy versus computer simulations. Biophy J. 2009; 96: 1105-1114.
    PubMed: https://www.ncbi.nlm.nih.gov/pubmed/19186146

17. Qin Z, Kreplak L, Buehler MJ. Nanomechanical properties of vimentin intermediate filament dimers. Nanotechnology. 2009; 20: 425101-425108.
    PubMed: https://www.ncbi.nlm.nih.gov/pubmed/19779230

18. Middelberg APJ, He L, Dexter AF, Shen HH, Holt SA, et al. The interfacial structure and Young's modulus of peptide films having switchable mechanical properties. J R Soc Interface. 2008; 5: 47-54.
    PubMed: https://www.ncbi.nlm.nih.gov/pubmed/17550885

19. Lei PF, Raae AJ, Altmann SM, Saraste M, Hörber JKH. States and transitions during forced unfolding of a single spectrin repeat. FEBS Lett. 2000; 476: 124-128.
    PubMed: https://www.ncbi.nlm.nih.gov/pubmed/10913598

20. Ogurtani TO. Mesoscopic nonequilibrium thermodynamics of solid surfaces and interfaces with triple junction singularities under the capillary and electromigration forces in anisotropic three-dimensional space. J Chem Phys. 2006; 124: 144706.
    PubMed: https://www.ncbi.nlm.nih.gov/pubmed/16626230

21. Ogurtani TO. Variational formulation of irreversible thermodynamics of surfaces and interfaces with grain-boundary triple junction singularities under the capillary and electromigration forces in anisotropic two-dimensional space. Phys Rev B. 2006; 73: 235408.

22. Ogurtani TO. Variational formulation of irreversible thermodynamics of isochoric and isobaric systems. 2015.

23. Hildebrand FB. Methods of applied mathematics. Prentice Hall, Englewood. 1961; 122.

24. Truesdell C. Thermodynamics of deformation, in nonequilibrium thermodynamics variational techniques and stability. Edited: R.J. Donnelly, R. Herman, I. Prigogine, Proceedings of Symposium, University of Chicago. 1965; 101-114.

25. Prigogine I, Int Thermodynamics of irreversible processes. Interscience Publ. 1955; 75.

26. De Groot SR. Thermodynamics of irreversible processes. North-Holland Co. Amsterdam. 1961; 22.

27. Ogurtani TO. Unified theory of linear instability of anisotropic surfaces and interfaces under capillary, electrostatic, and elastostatic forces: The regrowth of epitaxial amorphous silicon. Phys Rev B. 2006; 74: 1-23.

28. Ogurtani TO, Oren EE. Irreversible thermodynamics of triple junctions during the intergranular void motion under the electromigration forces. Int J Solids Structures. 2005; 42: 3918-3952.

29. Demaret JP, Gueron M. Composite cylinder models of DNA: Application to the electrostatic of B-Z transition. Biophys J. 1993; 65: 1700-1713.
PubMed: https://www.ncbi.nlm.nih.gov/pubmed/8274658

30. Weatherburn CE. Elementary Vector Analysis, with Application to Geometry and Mechanics. G Bell and Sons. 1955; 99-102.

31. Timoshenko S, Goodier JN. Theory of elasticity. McGraw-Hill New York. 1951; 361.

32. Cheatham TE, Case DA. Twenty-Five years of nucleic acid simulations. Biopolymers. 2013; 99: 969-977.
PubMed: https://www.ncbi.nlm.nih.gov/pubmed/23784813

33. Huang Y, Li L. DNA crosslinking damage and cancer-a table of friend and the foe. Transl Cancer Res. 2013; 2: 144-154.
PubMed: https://www.ncbi.nlm.nih.gov/pubmed/23998004

34. Allentoft ME, Collins M, Harker D, Haile J, Oskam CL, et al. The half-life of DNA in bone: measuring decay kinetics in 158 dated fossils. Proc Biol Sci. 2012; 279: 4724-4733.
PubMed: https://www.ncbi.nlm.nih.gov/pubmed/23055061

35. www.scientificamerican.com/.../oldest-ancient-human-dna-details-dawn. 2016.

36. Callaway E. 45,000 years old man's genome sequenced. Nature magazine. 2016.